Strangeness production in Pb-Pb collisions with ALICE at the LHC

Peter Kalinak[*] **for the ALICE collaboration**
Institute of Experimental Physics, Slovak Academy of Sciences, Kosice, Slovakia
E-mail: pkalinak@cern.ch

We present new ALICE results on the production of strange and multi-strange hadrons in Pb–Pb collisions at the top LHC energy of $\sqrt{s_{NN}}$ = 5.02 TeV. Strangeness production measurements are powerful tools for the study of the thermal properties of the deconfined state of QCD matter, the Quark-Gluon Plasma. Thanks to its unique tracking and PID capabilities, ALICE is able to measure weakly decaying particles through the topological reconstruction of the identified hadron decay products. Transverse momentum spectra of K^0_S, Λ, Ξ and Ω at central rapidity are presented as function of the collision centrality. The so-called baryon anomaly in the ratio Λ/K^0_S is examined to probe particle production mechanisms: the position of the peak is sensitive to recombination processes, the high-p_T part can provide revealing insights on fragmentation and, finally, the steepness of the rising trend featuring for $p_T \lesssim 2$ GeV/c can be connected to the hydrodynamic expansion of the system. In order to study strangeness enhancement, hyperon yields are normalised to the measurements of pion production in the corresponding centrality classes. Comparisons to lower energy results as well as to different collision systems will be shown. This offers a complete experimental picture that is used as a benchmark for commonly adopted phenomenological models, such as the thermal statistical hadronisation approach.

---

[*]Speaker.

1. Introduction

It is generally believed that Quantum Chromodynamics is correctly describing the strong interaction between hadrons. When the energy density of hadronic matter exceeds some typical hadronic value (~ 1 GeV/fm^3), matter undergoes the transition from the hadronic state to the state of quasi free quarks and gluons, the Quark Gluon Plasma (QGP) [1]. Probably the best way to create such a state in laboratory is by colliding highly-energetic heavy nuclei. In such a collision, the fast expanding, short living ($\sim 10^{-23}s$) fireball of hot QCD plasma is created [2]. Because the system expands rapidly, it cools down and distances between interacting partons increase. Quarks recombine to form hadrons and the system goes through a phase transition from QGP to hadronic gas. When the fireball is sufficiently diluted the inelastic collisions cease and the abundances of the produced particles are fixed. This is known as "chemical freeze-out" of the fireball. After further expansion also elastic collisions cease and the system undergoes the so called "kinematic freeze-out". Because the fireball expands and evolves through different stages after the phase transition, it is not trivial to acquire information about the QGP state of matter created shortly after the collision. One of the suggested ways to study the properties of the fireball is the measurement of strangeness production, and, in particular, of the so-called strangeness enhancement (relative to u and d quark production) with respect to elementary collisions. This enhancement was historically considered as a signature of QGP formation [3] and it was observed by several experiments [4–8], however the precise mechanism of strangeness production is not known. Canonical suppression and core-corona interplay are also considered as alternative explanations for strangeness enhancement [9].

2. Experimental setup

The ALICE detector has the capability to identify and measure charged particles, their trajectories and momenta in high energy heavy-ion collisions. The detector is surrounding the primary vertex where accelerated nuclei provided by the LHC collide. The central barrel tracking detectors are situated inside a solenoid magnet, which provides a uniform magnetic field of 0.5 T allowing for momentum measurement. To determine the centrality of a collision the ALICE experiment use V0 detectors situated on both sides of the interaction point in pseudorapidity regions $2.8 < \eta < 5.1$ and $-3.7 < \eta < -1.7$. The signal in V0 scintillators is proportional to the ionisation energy deposited in the detectors. This information is further used to to determine the centrality of the collision [10]. The two innermost central detectors, ITS (Inner Tracking System) and TPC (Time Projection Chamber) serve as tracking detectors. The ITS consists of three 2-layers silicon detectors. SPD (Silicon Pixel Detector), SDD (Silicon Drift Detector) and SSD (Silicon Strip Detector). The ITS provides a fast trigger signal, vertex reconstruction and particle identification. The TPC is a large cylindrical drift detector filled with a gas mixture (Ne 90% and CO_2 10%) used for particle trajectory reconstruction, particle identification and momentum measurement [11]. The new results on strangeness production at midrapidity ($|y|$<0.5) presented in this work are based on the analysis of a data sample of Pb–Pb collisions at $\sqrt{s_{NN}}$ = 5.02 TeV collected in 2015 during the Run 2 of the LHC. Data were collected using a minimum bias trigger (requiring a hit in both V0A and V0C scintillators). In total, a sample of 70 million events was analysed.

1

3. K_S^0, Λ, Ξ and Ω signal extraction in Pb–Pb at $\sqrt{s_{NN}}$ = 5.02 TeV

All considered particles are weakly decaying and their identification is indirect via their decay topology. In case of K_S^0 and Λ it is the so called V0 decay topology, in which the mother particle decays to oppositely charged particles with trajectories curved (in a magnetic field) in opposite directions in a shape of letter "V". Taking in to account the V0 topology parameters the V0 candidates are selected by means of a "V0 finder" algorithm looping over all reconstructed tracks. K_S^0 mesons are identified via the decay channel $K_S^0 \rightarrow \pi^+ + \pi^-$ with the branching ratio 69.2% and $\Lambda(\overline{\Lambda})$ hyperons are identified via the decay channel $\Lambda(\overline{\Lambda}) \rightarrow p(\overline{p}) + \pi^-(\pi^+)$ with the branching ratio 63.9%. In case of Ξ and Ω hyperons, the used decay channels are $\Xi^-(\overline{\Xi}^+) \rightarrow \Lambda(\overline{\Lambda}) + \pi^-(\pi^+)$ with the branching ratio 99.9% and $\Omega^-(\overline{\Omega}^+) \rightarrow \Lambda(\overline{\Lambda}) + K^-(K^+)$ with the branching ratio 67.8±0.7% . The signal is obtained by extracting the peak in the invariant mass distribution (fig. 1).
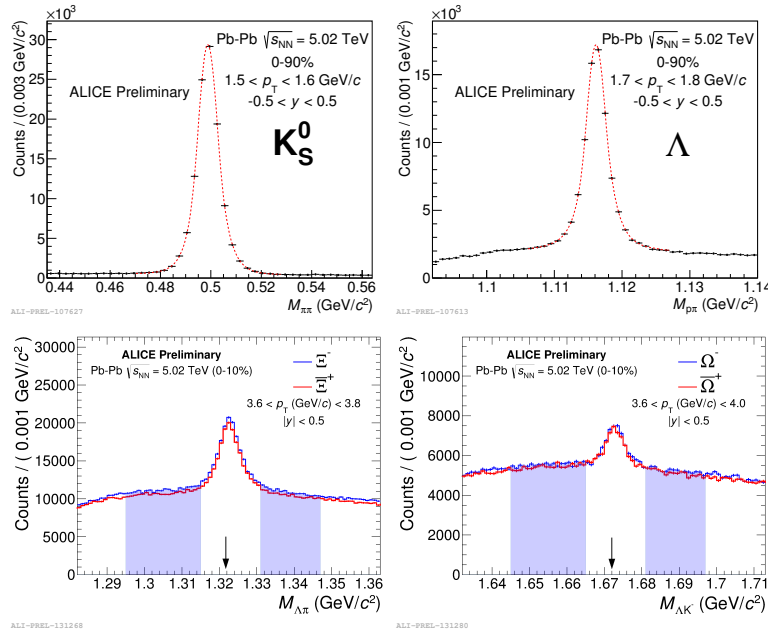
Figure 1: The invariant mass distribution for K_S^0 (upper left) in the transverse momentum interval $1.5 < p_T < 1.6$ GeV/c, Λ (upper right) in the transverse momentum interval bin $1.7 < p_T < 1.8$ GeV/c, Ξ^- $(\overline{\Xi}^+)$ in the transverse momentum interval $3.6 < p_T < 3.8$ GeV/c and $\Omega^+(\overline{\Omega}^-)$ in the transverse momentum interval $3.6 < p_T < 4$ GeV/c. Fitted are Gaussian plus polynomial functions used to describe the peak width and background. The arrow (lower row) indicates the position of peak resulting from the Gaussian fit and shaded areas shows the position of considered background regions.

4. Results

The p_T-differential yields are computed in ten centrality bins for K_S^0, Λ and $\overline{\Lambda}$, nine centrality bins for Ξ and seven centrality bins for Ω (fig. 2 and fig. 3). The number of p_T bins and p_T ranges vary with particle type and centrality due to limited statistic. Spectra are corrected for detector acceptance and reconstruction efficiency (also feeddown correction in case of Λ and $\overline{\Lambda}$).

Corrections were determined using Monte Carlo simulation, where events were generated with HIJING [12]. The hardening of the spectra with increasing centrality and particle mass is observed. A similar trend was observed also for the spectra measured in Pb–Pb collisions at $\sqrt{s_{NN}}$ = 2.76 TeV [8] [13].
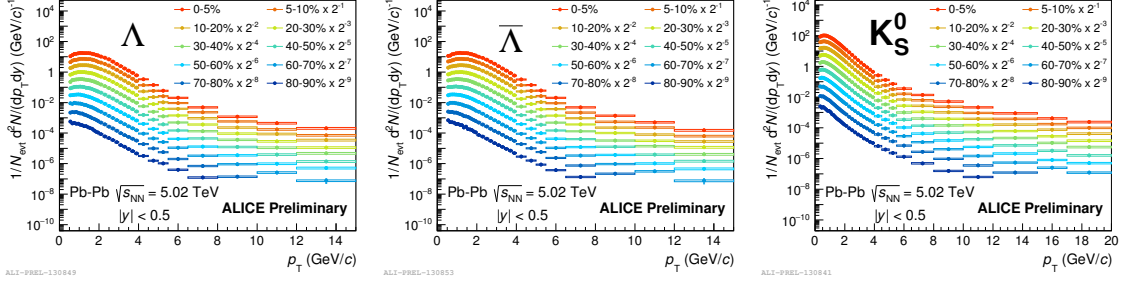
Figure 2: The p_T-differential yields for $\Lambda(\overline{\Lambda})$ and K_S^0 computed in ten centrality classes. The statistical errors are plotted as error bars and systematic uncertainties as boxes.
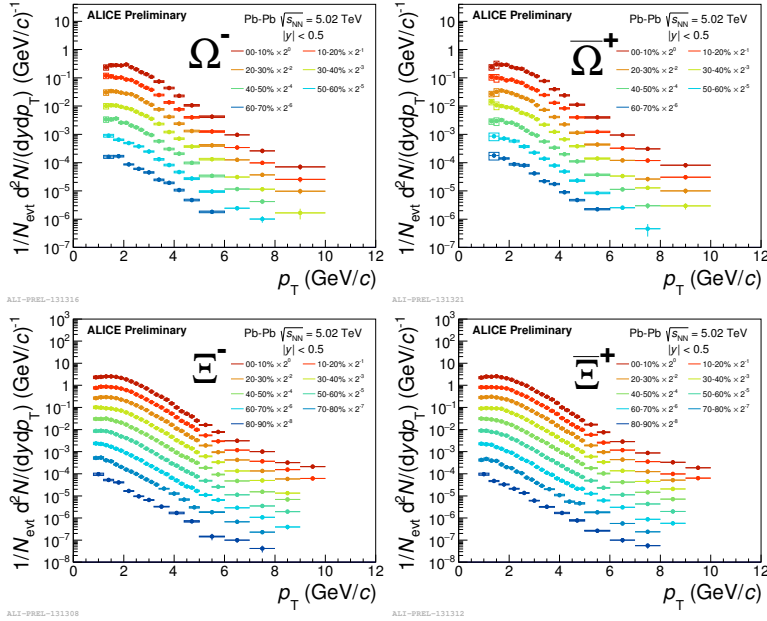
Figure 3: p_T-differential yields in seven centrality classes for $\Omega^+(\overline{\Omega}^-)$ and nine centrality classes for $\Xi^-(\overline{\Xi}^+)$. The statistical errors are plotted as error bars and systematic uncertainties as boxes.

The Λ/K_S^0 ratio is shown in five classes of centrality (fig. 4 left). For each class the correlation of systematic uncertainties between K_S^0 and Λ spectra was considered which reduced the final systematic uncertainty of the ratios (open boxes). The ratios follow a similar trend with centrality as the ones measured at $\sqrt{s_{NN}}$ = 2.76 TeV [13] (fig. 4 right). The peak height and position shifts toward higher values with increasing centrality of the collision and the centrality dependence of ratios diminishes below 2 GeV/c and above 7 GeV/c. The ALICE results for Pb–Pb at $\sqrt{s_{NN}}$

= 2.76 TeV were also compared to the measurements in Au–Au at $\sqrt{s_{NN}}$ = 0.2 TeV by STAR and model predictions. While the ALICE and STAR ratios are consistent in the most peripheral centrality class, in the most central class they differ for both, peak height and position. A good agreement with 2.76 TeV results for low p_T region is observed for hydrodynamical calculations for most central collision. Above 2 GeV/c EPOS gives better description of a data. In the p_T region above 6 GeV/c the recombination models seems to give good description but overpredicts the strangeness production in the mid-p_T region by ∼15%.
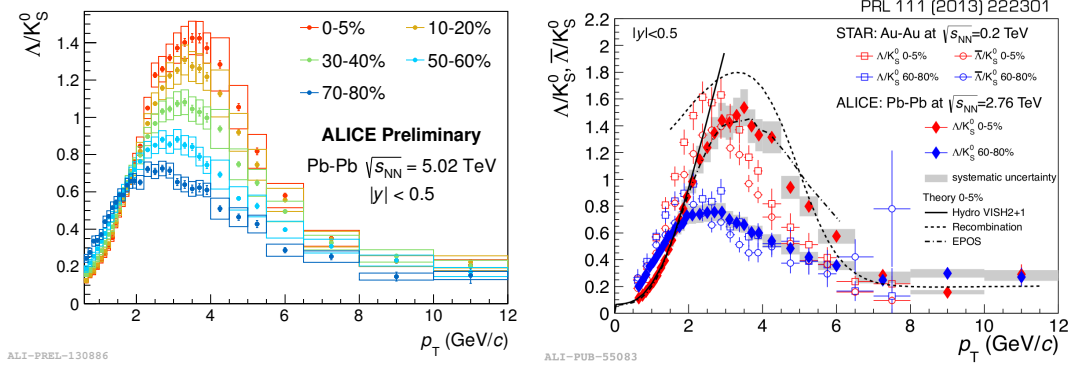
Figure 4: (Left) Λ/K_S^0 spectra ratios computed in five centrality classes. (Right) Λ/K_S^0 ratios in two centrality bins, measured by STAR collaboration in Au–Au collisions at $\sqrt{s_{NN}}$ = 0.2 TeV compared to the Λ/K_S^0 ratio in same centrality classes measured by ALICE collaboration in Pb–Pb collisions at $\sqrt{s_{NN}}$ = 2.76 TeV and to the models [13].
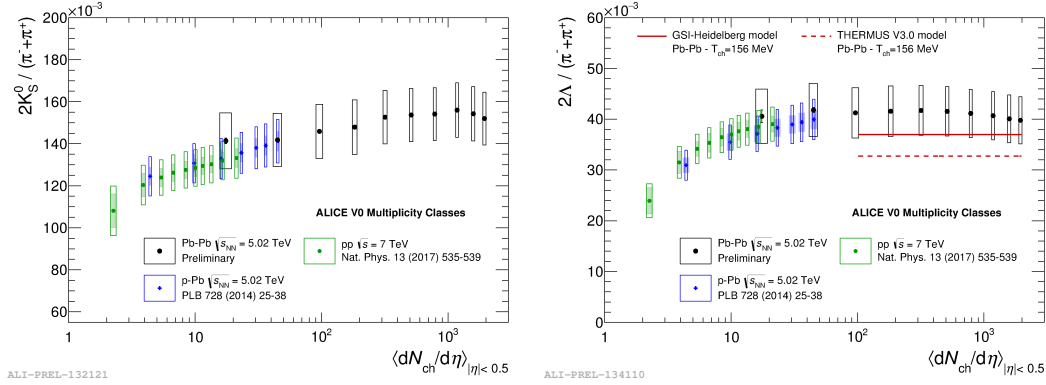
Figure 5: (Left) the ratio of integrated yields $2K_S^0/(\pi^+ + \pi^-)$ in the centrality classes measured in Pb–Pb collisions at $\sqrt{s_{NN}}$ = 5.02 TeV compared tho the same ratios measured in pp collisions $\sqrt{s}$ = 7 TeV and p–Pb collisions at $\sqrt{s_{NN}}$ = 5.02 TeV. (Right) The ratio of integrated yields $2\Lambda/(\pi^+ + \pi^-)$ in the centrality classes measured in Pb–Pb collisions at $\sqrt{s_{NN}}$ = 5.02 TeV compared to the same ratios measured in pp collisions $\sqrt{s}$ = 7 TeV and p–Pb collisions at $\sqrt{s_{NN}}$ = 5.02 TeV and to the prediction of GSI-Heidelberg [15] and THERMUS 2.3 [16] models represented by horizontal lines.

The integrated yields were computed for all particles under study in the centrality classes described above. In case of Λ, $\bar{\Xi}^+$, Ξ^-, $\bar{\Omega}^+$ and Ω^- lowest p_T bins starts above 0 and so the extrapolation of the spectra is needed to obtain complete. The spectra are extrapolated to zero using the function given by the Boltzmann-Gibbs Blast-Wave (BG-BW) model [14]. The systematic

uncertainty related to the extrapolation is computed using several alternative fit functions. The K_S^0 to π ($2K_S^0/(\pi^+ + \pi^-)$) ratios, Λ to π ($2\Lambda/(\pi^+ + \pi^-)$) ratios (fig. 5), Ξ to π (($\Xi^- + \bar{\Xi}^+)/(\pi^- + \pi^+)$) ratios and Ω to π (($\Omega^- + \bar{\Omega}^+)/(\pi^- + \pi^+)$) ratios (fig. 6) as a functions of $\langle dN_{ch}/d\eta \rangle$ are compared to the same ratios from pp collisions at $\sqrt{s}$ = 7 TeV and ratios from p–Pb collisions at $\sqrt{s_{NN}}$ = 5.02 TeV in order to study the relative production of strangeness. In all cases a smooth transition from small to large collision systems, and centralities is observed. The dependence of the hadron-to-pion yield on $\langle dN_{ch}/d\eta \rangle$ suggests the possible reach of the Grand Canonical limit in thermal particle production, especially in case of $2\Lambda/(\pi^+ + \pi^-)$ (fig. 5 right) for higher values of $\langle dN_{ch}/d\eta \rangle$.
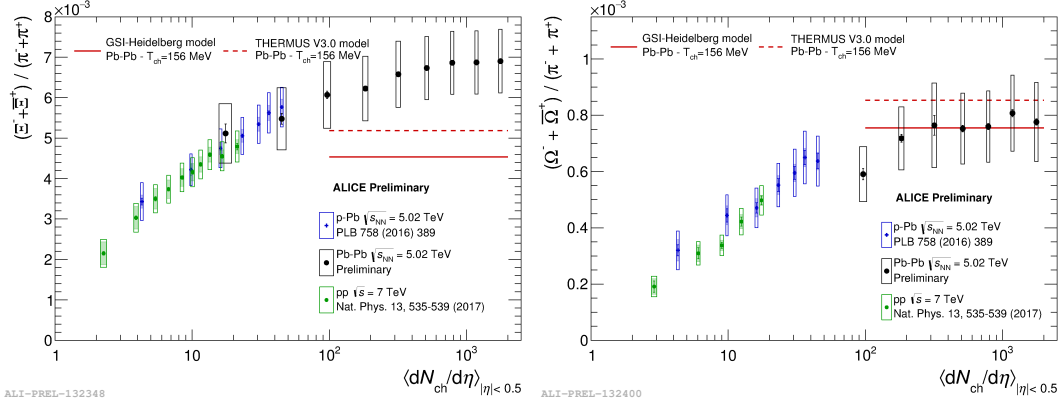
Figure 6: The ratio of integrated yields $(\Xi^- + \bar{\Xi}^+)/(\pi^- + \pi^+)$ in nine centrality classes (left) and $(\Omega^- + \bar{\Omega}^+)/(\pi^+ + \pi^-)$ in seven centrality classes (right) measured in Pb–Pb collisions at $\sqrt{s_{NN}}$ = 5.02 TeV compared to the same ratios measured in pp collisions $\sqrt{s}$ = 7 TeV and p–Pb collisions at $\sqrt{s_{NN}}$ = 5.02 TeV and to the prediction of GSI-Heidelberg [15] and THERMUS 2.3 [16] models represented by horizontal lines.

In case of Λ to π ratios (fig. 5 right), Ξ to π ratios (fig. 6 left) and Ω to π ratios (fig. 6 right) the $\langle dN_{ch}/d\eta \rangle$ dependencies are also compared to GSI-Heidelberg [15] and THERMUS 2.3 [16] thermal models. These predictions (horizontal lines) are obtained from the fit to to particle yields measured in Pb–Pb at 2.76 TeV and are in agreement within $\sim 1\sigma$ with Λ to π and Ω to π ratio measurements, however they do not describe the Ξ to π ratios with the same precision as for the other (multi-)strange particles and a difference of $\sim$ 2.1-2.8 σ between data and models is observed.

References

[1] E. V. Shuryak, "Quantum Chromodynamics and the Theory of Superdense Matter," Phys. Rept. 61(1980) 71-158.

[2] R. Anishetty, P. Koehler, and L. McLerran, " Central collisions between heavy nuclei at extremely high energies: The fragmentation region", Phys.Rev. D 22, 2793 (1980).

[3] J. Rafelski and B. Müller, "Strangeness production in the quark-gluon plasma," Phys. Rev. Lett. 48 (1982) 1066-1069. [Erratum Phys. Rev. Lett. 56 (1986) 2334-2334].

[4] WA97 Collaboration, E. Andersen et al., "Strangeness enhancement at mid-rapidity in Pb–Pb collisions at 158 AGeV/c," Phys. Lett. B449 (1999) 401-406.

[5] NA49 Collaboration, S. V. Afanasiev et al., "Ξ^- and $\bar{\Xi}^+$ production in central Pb+Pb collisions at 158 GeV/c per nucleon," Phys. Lett. B538 (2002) 275-281, arXiv:hep-ex/0202037 [hep-ex].

[6] NA57 Collaboration, F. Antinori et al., "Energy dependence of hyperon production in nucleus nucleus collisions at SPS," Phys. Lett. B595 (2004) 68-74, arXiv:nucl-ex/0403022 [nucl-ex].

[7] STAR Collaboration, B. I. Abelev et al., "Enhanced strange baryon production in Au+Au collisions compared to p+p at $\sqrt{s}$ = 200 GeV," Phys. Rev. C77 (2008) 044908, arXiv:0705.2511 [nucl-ex].

[8] ALICE Collaboration, B. Abelev et al., "Multi-strange baryon production at mid-rapidity in Pb–Pb collisions at $\sqrt{s_{NN}}$ = 2.76 TeV," Phys. Lett. B728 (2014) 216-227, arXiv:1307.5543[nucl-ex]. [Erratum: Phys. Lett. B734, 409 (2014)].

[9] F. Becattini and J. Manninen, "Strangeness production from SPS to LHC," J. Phys. G35 (2008)104013, arXiv:0805.0098 [nucl-th].

[10] ALICE Collaboration, B. Abelev et al., "Centrality determination of Pb–Pb collisions $\sqrt{s_{NN}}$ = 2.76 TeV with ALICE", Phys. Rev. C 88 (2013) 044909.

[11] ALICE Collaboration (Aamodt, K. et al.), "The ALICE experiment at the CERN LHC", JINST 3 (2008) S08002.

[12] X.-N. Wang and M. Gyulassy, "hijing: A Monte Carlo model for multiple jet production in pp, pA, and AA collisions ", Phys. Rev. D 44, 3501 (1991).

[13] ALICE Collaboration, B. Abelev et al., "K_S^0 and Λ production in Pb–Pb collisions at $\sqrt{s_{NN}}$ = 2.76 TeV", Phys. Rev. Lett. 111 (2013) 222301.

[14] E. Schnedermann, J. Sollfrank, and U. W. Heinz, "Thermal phenomenology of hadrons from 200A GeV S+S collisions," Phys. Rev. C 48 (1993) 2462-2475, arXiv:nucl-th/9307020.

[15] A. Andronic, P. Braun-Munzinger, and J. Stachel, "Thermal hadron production in relativistic nuclear collisions: The hadron mass spectrum, the horn, and the QCD phase transition," Physics Letters B 673 (2009) 142-145.

[16] S. Wheaton, J. Cleymans, and M. Hauer, "THERMUS - a thermal model package for ROOT," Computer Physics Communications 180 (2009) 84 - 106.

PoS(EPS-HEP2017)168